



Cite this article: Chen N *et al.* 2018 Atom economy and green elimination of nitric oxide using ZrN powders. *R. Soc. open sci.* **5**: 171516. <http://dx.doi.org/10.1098/rsos.171516>

Received: 30 September 2017

Accepted: 18 April 2018

Subject Category:

Chemistry

Subject Areas:

green chemistry/inorganic chemistry

Keywords:

green elimination, nitric oxide, zirconium nitride

Authors for correspondence:

Qiang Wang

e-mail: qwchem@gmail.com

Changzheng Wang

e-mail: changzhwang@163.com

Shaowei Chen

e-mail: shaowei@ucsc.edu

[†]These authors contributed equally to this work.

This article has been edited by the Royal Society of Chemistry, including the commissioning, peer review process and editorial aspects up to the point of acceptance.



Atom economy and green elimination of nitric oxide using ZrN powders

Ning Chen¹, Jigang Wang¹, Wenyan Yin², Zhen Li¹, Peishen Li¹, Ming Guo¹, Qiang Wang^{1,†}, Chunlei Li¹, Changzheng Wang^{3,†} and Shaowei Chen^{4,†}

¹Laboratory for Micro-sized Functional Materials and College of Elementary Education and Department of Chemistry, Capital Normal University, Beijing, 100048, People's Republic of China

²Key Laboratory for Biomedical Effects of Nanomaterials and Nanosafety Institute of High Energy Physics, Chinese Academy of Sciences, Beijing, 100049, People's Republic of China

³Beijing Key Laboratory of Functional Materials for Building Structure and Environment Remediation, Beijing University of Civil Engineering and Architecture, Beijing, 100044, People's Republic of China

⁴Department of Chemistry and Biochemistry, University of California, 1156 High Street, Santa Cruz, CA 95064, USA

NC, 0000-0002-9355-6993

Nitric oxide (NO) may cause serious environmental problems, such as acid rain, haze weather, global warming and even death. Herein, a new low-cost, highly efficient and green method for the elimination of NO using zirconium nitride (ZrN) is reported for the first time, which does not produce any waste or any by-product. Relevant experimental parameters, such as reaction temperature and gas concentration, were investigated to explore the reaction mechanism. Interestingly, NO can be easily decomposed into nitrogen (N₂) by ZrN powders at 600°C with ZrN simultaneously transformed into zirconium dioxide (ZrO₂) gradually. The time for the complete conversion of NO into N₂ was approximately 14 h over 0.5 g of ZrN at a NO concentration of 500 ppm. This green elimination process of NO demonstrated good atom economy and practical significance in mitigating environmental problems.

1. Introduction

Emission of nitrogen oxides (NO_x) produced from stationary and mobile combustion sources is one of the major contributors to atmospheric contamination [1]. In fact, NO_x has been known to lead to worsening of local air quality, regional acid rain pollution as well as photochemical smog [2,3]

and undesirable severe damage to human health [4]. With increasingly stringent NO_x emission regulations, extensive efforts have been devoted to the development of new technologies for the elimination of NO_x emission. Catalytic oxidation of nitric oxide (NO) plays a critical role in NO_x storage and reduction [5,6]; and continuously regenerating trap [7] and selective catalytic reduction (SCR) [8–10] have been the main technologies for NO_x removal. Among these, catalytic oxidation based on CuO_x/Al₂O₃ and CuO_x/LaO_x/Al₂O₃ has been widely used in the treatment of automobile exhaust, which typically operates in the temperature range of 200–400°C [11], yet only less than 50% of NO can be eliminated. Note that for gasoline vehicles, the exhaust gas temperature may be up to 1000°C, which can lead to deactivation of the catalysts. SCR is of particular interest because it has been successfully employed for the reduction of NO_x by NH₃: $4\text{NO} + 4\text{NH}_3 + \text{O}_2 = 4\text{N}_2 + 6\text{H}_2\text{O}$. However, the use of ammonia increases the cost of operation and raises safety issues due to its corrosive nature. Furthermore, in the SCR reaction, NO and ammonia are introduced into the reaction vessel at a 1 : 1 molar ratio, and at insufficient reactants, there may be an outflow of excess ammonia, resulting in secondary pollution. Therefore, it is urgently needed to develop 'green' and thermostable procedures for the treatment of gasoline vehicle exhaust especially for the removal of NO_x.

Within this context, transition metal nitrides (e.g. TiN, GaN, etc.) have been attracting attention as viable candidates for NO_x removal, although they are better known for improving the lifetime and performance of cutting tools [12,13]. Among these, zirconium nitride (ZrN) has been extensively studied owing to its excellent physicochemical and tribological properties [14,15]. For instance, ZrN possesses high hardness, good electrical conductivity and low chemical reactivity [16], and has been used as wear resistant coatings on cutting tools [17], and as decorative films for scratch resistance and colouring in the jewellery industry [18]. Thin films of ZrN have also been used as diffusion barriers in integrated circuits [19]. However, up to now, reports have remained scarce involving the application of ZrN for the elimination of pollution gases. Currently, the synthetic methods of ZrN mainly include reactive magnetron sputtering, gas–solid reaction and physical vapour deposition-based methods [20,21], such as pulsed laser deposition [22,23], chemical beam epitaxy [24], ion plating [25] and vacuum evaporation [26]. Among these methods, gas–solid method is the most simple and economical.

In this study, ZrN powders were synthesized by gas–solid reactions of Zr powders under a N₂ gas-flow and demonstrated apparent reactivity in the reduction of NO by the following reaction: $2\text{ZrN} + 4\text{NO} = 2\text{ZrO}_2 + 3\text{N}_2$. In a typical experiment, 0.5 g of ZrN powder was sufficient for complete reduction of 500 ppm NO gas for up to 14 h at 600°C. The *in vitro* cytotoxicity evaluation and haemolysis assays have shown that the reaction product, zirconium dioxide (ZrO₂), may be used as a biocompatible material for bone tissue engineering and regenerative medicine [27] and the other reaction product, N₂, may be used as a protective gas or converted into liquid nitrogen for other purposes. In addition, no ammonia was used and there was no concern of corrosion for the reaction apparatus as well as secondary pollution. This suggests that the reaction process is atom economy and green chemistry in nature. Importantly, as NO was effectively removed at elevated temperatures, the results suggest that ZrN may be used as a green catalyst for gasoline vehicle exhaust treatment that runs at harsh high temperatures.

2. Experimental

2.1. Material preparation

All chemicals were purchased from Alfa Aesar and used as received without further purification. To prepare ZrN, zirconium powders were placed in a square boat and heated at 1200°C in a corundum tube under nitrogen for 12 h [28].

2.2. Material characterizations

The phase structures and morphologies of the ZrN powders prepared above were characterized by powder X-ray diffraction (XRD, Bruker D8 with Cu K α radiation, $\lambda = 1.54 \text{ \AA}$) and X-ray photoelectron spectroscopy (XPS, ESCALAB 250 with Al K α radiation) measurements. The lattice fringes of the obtained samples and the corresponding selected-area electron diffraction (SAED) patterns were examined by using a high-resolution transmission electron microscope (HRTEM, JEOL 2010F, 200 kV).

2.3. Elimination reduction of nitric oxide

Elimination reduction of NO was performed in a fixed-bed quartz tube reactor with an internal diameter of 6 mm [29]. The ZrN powders were ground to 40–60 mesh and placed on quartz wool held in the reactor, and the reactor was heated by a vertical electrical furnace. The total flow rate was 250 ml min⁻¹ (room temperature), the mass of ZrN was 500 mg, and the corresponding gas hourly space velocity was $10 \times 10^4 \text{ cm}^3 \text{ g}^{-1} \text{ h}^{-1}$, which was evaluated by the following expression:

$$\text{GHSV} = \frac{q_v}{\pi h r^2}, \quad (2.1)$$

where q_v is the total flow rate, h is the height of the reactant in the reactor and r is the radius of the reactor [30]. The concentration of NO was monitored by an online gas chromatographic analyser equipped with a flame photometric detector (Beijing Beifen-Ruili 3420A). The NO conversion ratio was calculated by the following equation [31]:

$$\text{NO}_{\text{conversion}} = \frac{[\text{NO}]_{\text{in}} - [\text{NO}]_{\text{out}}}{[\text{NO}]_{\text{in}}} \times 100\%, \quad (2.2)$$

where $[\text{NO}]_{\text{in}}$ and $[\text{NO}]_{\text{out}}$ refer to the NO concentration at the inlet and outlet, respectively.

3. Results and discussion

3.1. X-ray photoelectron spectroscopy characterization

The as-prepared ZrN sample was characterized by XPS measurements. From the survey spectrum (figure 1a), one can readily identify Zr 3s electrons at 421.36 eV, Zr 3d electrons at 181.72 and 183.65 eV, Zr 4s electrons at 58.31 eV, Zr 4p electrons at 33.15 eV and N 1s electrons at 396.38 eV (the O 1s electrons at 529.15 eV suggests surface partial oxidation, whereas the C 1s electron at 179.25 eV likely arose from residual carbon). In fact, high-resolution scans show a doublet at 181.72 and 183.65 eV for the Zr 3d electrons (figure 1b) and N 1s electrons at 396.38 eV (figure 1c), consistent with those of ZrN [32]. Furthermore, based on the integrated peak areas, the mole ratio of Zr/N is estimated to be 1 : 0.87, which is close to that of ZrN.

3.2. Powder X-ray diffraction characterization

XRD measurements of the ZrN sample (figure 2) show five well-defined diffraction peaks, which correspond to a d-spacing of 2.6310, 2.2799, 1.6145, 1.3779 and 1.3191 Å, and can be indexed to the (111), (200), (220), (311) and (222) crystalline planes of cubic phase ZrN (space group Fm $\bar{3}$ m, no. 225). The lattice constant of $a = 4.5675 \text{ \AA}$ is in good agreement with the JCPDS card no. 35-0753 [33–34]. This suggests that the produced ZrN powders possessed good crystallinity.

3.3. Transmission electron microscopy characterization

To elucidate the microscopic structure of the ZrN sample, we conducted a detailed TEM investigation. Figure 3 depicts two representative TEM micrographs at different magnifications. From figure 3a, it can be found that the morphology of the ZrN was of irregular particles with a diameter of 250–300 nm and a thickness of 20–30 nm. The corresponding HRTEM image is shown in figure 3b, which exhibited well-defined lattice fringes with two interplanar distances of 0.17 and 0.23 nm, corresponding to the (220) and (200) crystalline planes in cubic ZrN at a crossing angle of approximately 45°. The corresponding SAED pattern (inset to figure 3b) is also in good agreement with crystalline cubic ZrN [35].

3.4. Elimination reduction of nitric oxide

Figure 4 depicts the removal of NO by ZrN at different reaction temperatures. Experimentally, a gas containing 500 ppm NO balanced with N₂ was introduced into the reactor after 126 min, and the reaction was performed at different temperatures. One can see that with the increase of reaction temperature from 400 to 600°C, the efficiency of NO conversion over ZrN increased markedly (figure 4). Note that at 400°C, the concentration of NO at the outlet was equal to that at the inlet, suggesting no reactivity at this temperature. When the reaction temperature was increased to 500°C, the amount of NO detected at the outlet decreased slightly, indicating partial reduction of NO by ZrN. When the temperature was further

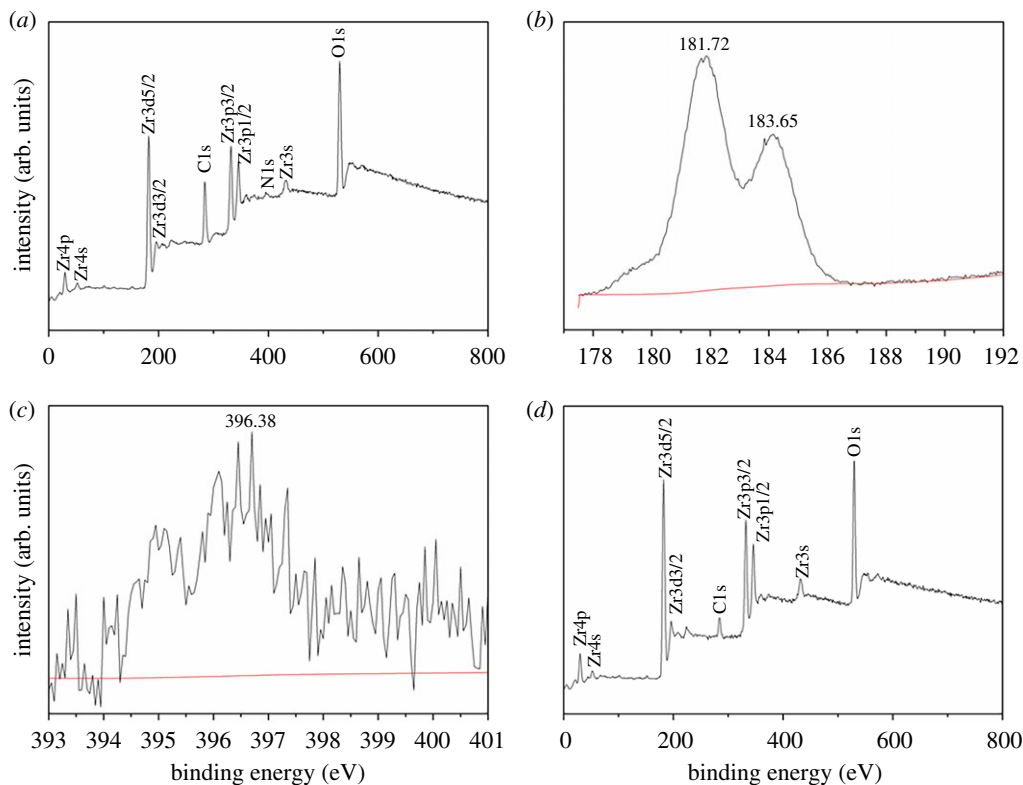


Figure 1. XPS analyses of the as-prepared ZrN sample and reaction product of ZrN and NO at 600°C. (a) Survey spectrum of ZrN, (b) Zr3d region of ZrN, (c) N1s region of ZrN and (d) survey spectrum of the reaction product after the reaction of ZrN and NO at 600°C.

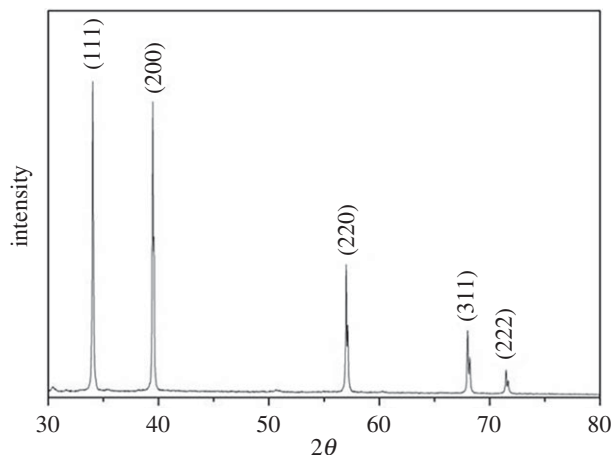


Figure 2. XRD pattern of the as-prepared ZrN sample.

raised to 600°C, no NO was detected at the outlet, indicating that NO was completely reduced by ZrN in the reactor. The conversion rate of NO in this reaction is much better than those reported with other catalysts such as $\text{CuO}_x/\text{Al}_2\text{O}_3$ and $\text{CuO}_x/\text{LaO}_x/\text{Al}_2\text{O}_3$ [11], suggesting that ZrN can be used in gasoline vehicle exhaust treatment at high temperatures.

Consistent results were obtained in XRD measurements of the solids before and after NO reaction (figure 5). When the reaction was carried out at 400°C, no variation of the diffraction patterns of the solids was observed, in agreement with the lack of chemical reactivity at this temperature. When the reaction temperature was raised to 500°C, the solids were found to consist of a mixture of ZrN and ZrO_2 , indicating that part of the ZrN was oxidized into ZrO_2 during the reduction of NO to N_2 . At the even higher reaction temperature of 600°C, no ZrN was detected and only ZrO_2 diffraction peaks were

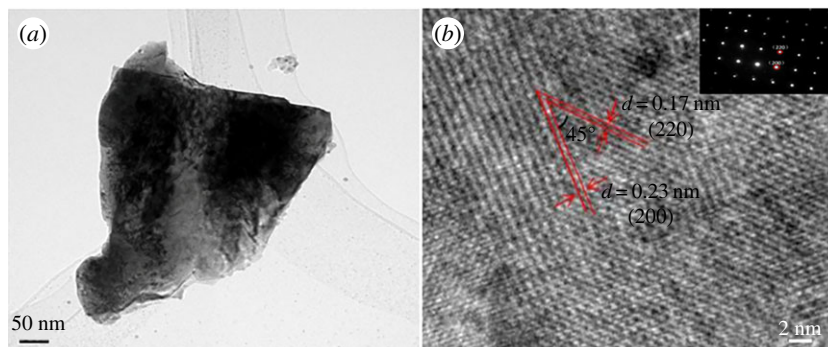


Figure 3. (a) TEM and (b) HRTEM images of the as-prepared ZrN. Inset to panel (b) is the corresponding SAED pattern.

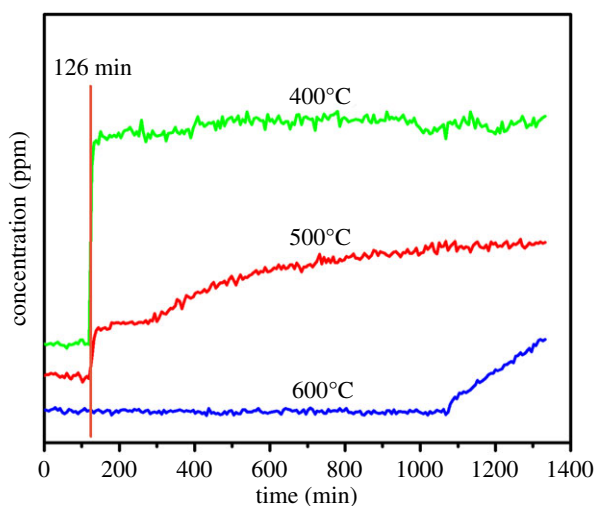


Figure 4. Degree of NO removal by ZrN at different reaction temperatures.

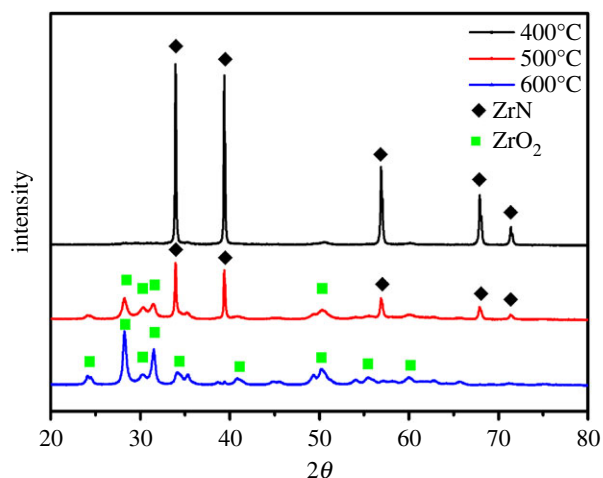


Figure 5. XRD patterns of the solids after NO reduction reaction at different temperatures.

observed. Consistent results were obtained in XPS measurements of the solids after reaction (figure 1d), due to complete consumption of ZrN in the reduction of NO: $2\text{ZrN} + 4\text{NO} = 2\text{ZrO}_2 + 3\text{N}_2$.

In further studies, reduction of NO by ZrN was carried out at 600°C with different concentrations of NO gas (500, 800 and 1000 ppm), where the gas was introduced into the reactor after 174 min, as

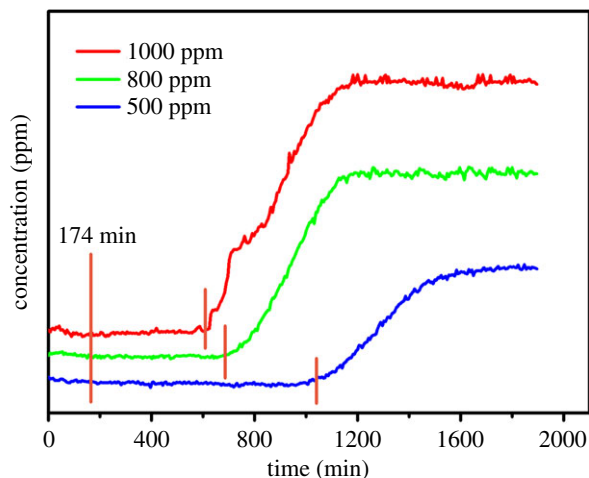


Figure 6. Reaction curves of ZrN with different concentrations of NO at 600°C.

depicted in figure 6. We can clearly see that at the gas concentration of 500 ppm, the amount of the added ZrN was sufficient to completely reduce NO for about 14 h. At increasing NO concentrations, the period of time where complete reduction of NO occurred was shortened accordingly. For instance, when the gas concentration increased to 800 and 1000 ppm, the operation time was shortened to 8.4 and 7.5 h, respectively.

4. Conclusion

In summary, ZrN powders were prepared by thermal treatment of Zr in a N₂ atmosphere at elevated temperatures, and exhibited apparent activity in the reduction of NO to N₂ where ZrN was oxidized to ZrO₂. The experimental results show that 0.5 g of ZrN powders was sufficient for complete reduction of 500 ppm NO gas for 14 h at 600°C, whereas the chemical reactivity diminished with decreasing temperature. The reaction products were detected as ZrO₂ and N₂, both of which are of practical value and cause no secondary pollution to the environment. Importantly, because of the high conversion rate of NO at elevated operation temperature, ZrN may be used as an effective substitute of conventional catalysts in the treatment of gasoline vehicle exhaust gas. These results highlight a new, unique approach based on the concept of green chemistry for the effective elimination of NO_x pollutants.

Data accessibility. All data generated or analysed during this study are included in this article.

Authors' contributions. N. C., J.-G.W. and W.-Y.Y. conducted the experiment, J.-G.W. and Z.L. wrote the manuscript. P.-S.L., M.G., Q.W., C.-Z.W., C.-L.L., C.-H.L. and S.-W. C. discussed and reviewed the manuscript.

Conflict of interest. The authors declare no conflict of interest.

Funding. This work was supported by the Natural Science Foundation of China (nos. 21471103, 51002180, 11275218 and 11574173), National Basic Research Programs of China (nos. 2016YFA0201603, 2015CB932104), Beijing Natural Science Foundation (no. 2162046) and the General Program of Science and Technology Development Project of Beijing Municipal Commission of Education (no. KM201410028021) and the Scientific Research Base Development Program of the Beijing Municipal Commission of Education (no. 203175302200).

Acknowledgements. We thank Mr Xiuhui Bai from Capital Normal University and Fengnan Yang from Beijing University of Civil Engineering and Architecture for helpful discussions.

References

- Klose W, Rincón S. 2007 Adsorption and reaction of NO on activated carbon in the presence of oxygen and water vapour. *Fuel* **86**, 203–209. (doi:10.1016/j.fuel.2006.06.017)
- Cai SX, Liu J, Zha KW, Li HR, Shi LY, Zhang DS. 2017 A general strategy for the in situ decoration of porous Mn-Co bi-metal oxides on metal mesh/foam for high performance de-NO_x monolith catalysts. *Nanoscale* **9**, 5648–5657. (doi:10.1039/c6nr09917c)
- Ramírez-Garza RE, Rodríguez-Iznaga I, Simakov A, Fariás MH, Castellón-Barraza FF. 2018 Cu-Ag/mordenite catalysts for NO reduction: effect of silver on catalytic activity and hydrothermal stability. *Mater. Res. Bull.* **97**, 369–378. (doi:10.1016/j.materresbull.2017.09.001)
- Zha KW, Cai SX, Hu H, Li HR, Yan TT, Shi LY, Zhang DS. 2017 In situ DRIFTS investigation of promotional effects of tungsten on MnO_x-CeO₂/meso-TiO₂ catalysts for NO_x reduction. *J. Phys. Chem. C* **121**, 25 243–25 254. (doi:10.1021/acs.jpcc.7b08600)
- Zhao DY *et al.* 2018 Addition of Pd on La_{0.7}Sr_{0.3}CoO₃ perovskite to enhance catalytic removal of NO_x. *Ind. Eng. Chem. Res.* **57**, 521–531. (doi:10.1021/acs.iecr.7b04399)
- Liu ZQ, Epling WS, Anderson JA. 2011 Influence of Pt loading in aged NO_x storage and reduction

- catalysts. *J. Phys. Chem. C* **115**, 952–960. (doi:10.1021/jp1040037)
7. Liu ZH, Ge YS, Tan JW, He C, Shah AN, Ding Y, Yu LX, Zhao W. 2012 Impacts of continuously regenerating trap and particle oxidation catalyst on the NO₂ and particulate matter emissions emitted from diesel engine. *J. Environ. Sci.* **24**, 624–631. (doi:10.1016/S1001-0742(11)60810-3)
 8. Yan LJ, Liu YY, Zha KW, Li HR, Shi LY, Zhang DS. 2017 Scale-activity relationship of MnO_x-FeO_y nanocage catalysts derived from Prussian blue analogues for low-temperature NO reduction: experimental and DFT studies. *ACS Appl. Mater. Interfaces* **9**, 2581–2593. (doi:10.1021/acsami.6b15527)
 9. Wang JP, Yan Z, Liu LL, Chen Y, Zhang ZT, Wang XD. 2014 In situ DRIFTS investigation on the SCR of NO with NH₃ over V₂O₅ catalyst supported by activated semi-coke. *Appl. Surf. Sci.* **313**, 660–669. (doi:10.1016/j.apsusc.2014.06.043)
 10. Zhong Q, Zhang TJ, Li YT, Ma WH, Qu HX. 2011 NO (or NH₃) + O₂ adsorption on fluorine-doped vanadia/titania and its role in the mechanism of a two-step process characterized by EPR. *Chem. Eng. J.* **174**, 390–395. (doi:10.1016/j.cej.2011.09.015)
 11. Masakuni O. 2006 Thermal stabilization of catalytic compositions for automobile exhaust treatment through rare earth modification of alumina nanoparticle support. *J. Alloys Compd.* **408–412**, 1090–1095. (doi:10.1016/j.jallcom.2004.12.111)
 12. Mitterer C, Holler F, Reitberger D, Badisch E, Stoiber M, Lugmair C, Nöbauer R, Müller T, Kullmer R. 2003 Industrial applications of PACVD hard coatings. *Surf. Coat. Technol.* **163**, 716–722. (doi:10.1016/S0257-8972(02)00685-0)
 13. Veprek S, Veprek-Heijman M.J.G. 2008 Industrial applications of superhard nanocomposite coatings. *Surf. Coat. Technol.* **202**, 5063–5073. (doi:10.1016/j.surfcoat.2008.05.038)
 14. Constantin R, Miremad B. 1999 Performance of hard coatings, made by balanced and unbalanced magnetron sputtering, for decorative applications. *Surf. Coat. Technol.* **120**, 728–733. (doi:10.1016/S0257-8972(99)00366-7)
 15. Ramana JV, Kumar S, David C, Ray AK, Raju VS. 2000 Characterisation of zirconium nitride coatings prepared by DC magnetron sputtering. *Mater. Lett.* **43**, 73–76. (doi:10.1016/S0167-577X(99)00233-5)
 16. Wu ZT, Qi ZB, Jiang WF, Wang ZC, Liu B. 2014 Influence of niobium addition on microstructure, mechanical properties and oxidation resistance of ZrN coatings. *Thin Solid Films* **570**, 256–261. (doi:10.1016/j.tsf.2014.05.019)
 17. Memagh VA, Kelly TC, Ahern M, Kennedy AD, Adriaansen AP, Ramaekers PP, McDonnell L, Koekoek R. 1991 Adhesion improvements in silicon carbide deposited by plasma enhanced chemical vapour deposition. *Surf. Coat. Technol.* **49**, 462–467. (doi:10.1016/0257-8972(91)90101-2)
 18. Beck U, Reiners G, Urban I, Jehn HA, Kopacz U, Schack H. 1993 Decorative hard coatings: new layer systems without allergy risk. *Surf. Coat. Technol.* **61**, 215–222. (doi:10.1016/0257-8972(93)90228-G)
 19. Wittmer M. 1980 High-temperature contact structures for silicon semiconductor devices. *Appl. Phys. Lett.* **37**, 540–542. (doi:10.1063/1.91978)
 20. Dauchot JP, Gouttebaron R, Wautelet M, Hecq M. 2000 Rapid growth of hard and compact layers of stoichiometric ZrN by DC reactive magnetron sputtering pulsed at low frequency. *Adv. Eng. Mater.* **2**, 824–827. (doi:10.1002/1527-2648(200012)2:12<824::AID-ADEM824>3.0.CO;2-I)
 21. Upadhyay RK, Kumaraswamidhas LA. 2016 Friction and wear response of nitride coating deposited through PVD magnetron sputtering. *Tribol. Mater. Surf. Interfaces* **10**, 196–205. (doi:10.1080/17515831.2016.1260791)
 22. Edward GG, Richard BK. 1994 Rapid solid-state synthesis of refractory nitrides. *Inorg. Chem.* **33**, 5693–5700. (doi:10.1021/ic00103a015)
 23. Hector AL, Henshaw G, Komarov AV, Parkin IP. 1998 Nitrides from solid state metathesis reactions: synthesis and mechanistic. *J. Mater. Process. Technol.* **77**, 103–107. (doi:10.1016/S0924-0136(97)00405-6)
 24. El-Eskandarany MS, Ashour AH. 2000 Mechanically induced gas–solid reaction for the synthesis of nanocrystalline ZrN powders and their subsequent consolidations. *J. Alloys Compd.* **313**, 224–234. (doi:10.1016/S0925-8388(00)01175-0)
 25. Narula CK. 1998 Novel zirconium nitride precursor: synthesis, decomposition pathway, and pyrolysis of [(CH₃)₃Si]₂NH•ZrCl₄. *J. Mater. Chem.* **8**, 1881–1884. (doi:10.1039/A802864H)
 26. Lerch M, Füglein E, Wrba J. 1996 Synthesis, crystal structure, and high temperature behavior of Zr₃N₄. *Z. Anorg. Allg. Chem.* **622**, 367–372. (doi:10.1002/zaac.1996622027)
 27. Wang JG, Yin WY, He X, Wang Q, Guo M, Chen SW. 2016 Good biocompatibility and sintering properties of zirconia nanoparticles synthesized via vapor-phase hydrolysis. *Sci. Rep.* **6**, 35020. (doi:10.1038/srep35020)
 28. Baker TW. 1955 The coefficient of thermal expansion of zirconium nitride. *Natl Geogr. Soc. India* **264**, 300. (doi:10.1107/S0365110X58000724)
 29. Lengauer W, Etmayer P. 1986 Lattice parameters and thermal expansion of δ-VN_{1-x} from 298–1000 K. *Monatsh. Chem.* **117**, 713–719. (doi:10.1007/BF0081006)
 30. Ole B, Juhl CJ, Niels H. 1976 The photocycloaddition of cyclohexene to carbostyrlis. *Acta Chem. Scand.* **30**, 189–192. (doi:10.3891/acta.chem.scand.30b-0189)
 31. Guan HL, Lin J, Li L, Wang XD, Zhang T. 2016 Highly active subnano Rh/Fe(OH)₃ catalyst for preferential oxidation of CO in H₂-rich stream. *Appl. Catal. B* **184**, 299–308. (doi:10.1016/j.apcatb.2015.11.040)
 32. Muneshwar T, Cadien K. 2018 Comparing XPS on bare and capped ZrN films grown by plasma enhanced ALD: effect of ambient oxidation. *Appl. Surf. Sci.* **435**, 367–376. (doi:10.1016/j.apsusc.2017.11.104)
 33. Wang LG, Tang HQ, Tian Y. 2016 Carbon-shell-decorated p-semiconductor PbMoO₄ nanocrystals for efficient and stable photocathode of photoelectron chemical water reduction. *J. Power Sources* **319**, 210–218. (doi:10.16/j.jpowsour.2016.04.059)
 34. Yin WY *et al.* 2014 High-throughput synthesis of single-layer MoS₂ nanosheets as a near-infrared photothermal-triggered drug delivery for effective cancer therapy. *ACS Nano* **8**, 6922–6933. (doi:10.1021/nn501647j)
 35. Zhao X, Huang L, Namuangruk S, Hu H, Hu XN, Shi LY, Zhang DS. 2016 Morphology-dependent performance of Zr-CeVO₄/TiO₂ for selective catalytic reduction of NO with NH₃. *Catal. Sci. Technol.* **6**, 5543–5553. (doi:10.1039/c6cy00326e)